Global Biogeochemical Cycles

RESEARCH ARTICLE
10.1029/2018GB005977

The Fate of Carbon and Nutrients Exported Out of the Southern Ocean

Judith Hauck[1], **Andrew Lenton**[2,3,4], **Clothilde Langlais**[2], **and Richard Matear**[2]

[1] Alfred Wegener Institut, Helmholtz Zentrum für Polar- und Meeresforschung, Bremerhaven, Germany, [2] CSIRO Oceans and Atmosphere, Hobart, TAS, Australia, [3] Centre for Southern Hemisphere Oceans Research, Hobart, TAS, Australia, [4] Antarctic Climate and Ecosystems Cooperative Research Centre, Hobart, TAS, Australia

Key Points:
- The Southern Ocean biological carbon pump has longer sequestration time scale than physical pump

Supporting Information:
- Supporting Information S1

Correspondence to:
J. Hauck,
judith.hauck@awi.de

Citation:
Hauck, J., Lenton, A. A., Langlais, C., & Matear, R. J. (2018). The fate of carbon and nutrients exported out of the Southern Ocean. *Global Biogeochemical Cycles*, *32*, 1556–1573. https://doi.org/10.1029/2018GB005977

Received 4 MAY 2018
Accepted 22 SEP 2018
Accepted article online 26 SEP 2018
Published online 26 OCT 2018

Abstract Southern Ocean (SO) nutrient export via mode and intermediate waters is known to affect global biological production. The accompanying effects on the CO_2 flux outside the SO are less certain. We performed idealized model simulations to separate the transient effects of SO carbon pumps on nutrients, primary production, and CO_2 flux outside the SO. The SO biological carbon pump leads to dissolved inorganic carbon and nutrient reduction at the surface and in the exported water masses, and to a dissolved inorganic carbon increase at depth through the sinking of organic matter. When primary production is suppressed in the SO, only 30% of SO export, 43% of SO net primary production, and 50% of biologically driven SO CO_2 flux are compensated outside the SO on a 200-year time scale. In contrast, when the abiotically driven CO_2 flux is suppressed, 90% of CO_2 outgassing in the SO is compensated by air-sea CO_2 exchange outside the SO. The longer sequestration time scale of the biological carbon pump can be explained by incomplete compensation of primary production. This is a result of almost complete compensation of diatom productivity and no compensation of nanophytoplankton productivity due to feedbacks in phytoplankton community composition. The longer sequestration time scale is further sustained by the sinking and remineralization of particles in the deep ocean that are not in contact with the atmosphere over the 200-year time scale considered. As SO biologically driven CO_2 flux is only partly compensated outside the SO, potential future changes in SO productivity may have an important impact on the global carbon cycle.

1. Introduction

The Southern Ocean (SO) south of 40°S covers 21% of the ocean surface area, but it is responsible for 40% of anthropogenic carbon (C_{ant}) uptake by the global ocean (Khatiwala et al., 2009). The C_{ant} uptake occurs mostly south of 40°S, where upwelling brings deep water, uncontaminated with C_{ant}, to the surface (Frölicher et al., 2015; Mikaloff Fletcher et al., 2006; Morrison et al., 2015). In contrast, the peak in the C_{ant} inventory reaches as far north as 20°S (Frölicher et al., 2015; Ito et al., 2010; Khatiwala et al., 2009). Northward Ekman transport of surface water, partially offset by eddies (Ito et al., 2010), carries the C_{ant} away from the uptake region (Frölicher et al., 2015; Mikaloff Fletcher et al., 2006). Formation and subduction of Subantarctic Mode Water (SAMW) and Antarctic Intermediate Water (AAIW; Sallée et al., 2012) transport C_{ant} into the ocean interior and contain more than half of the C_{ant} stored south of 30°S (Langlais et al., 2017).

The SO has changed from a preindustrial source of CO_2 to the atmosphere (Hoppema, 2004; Mikaloff Fletcher et al., 2007) to a contemporary CO_2 sink (Gruber et al., 2009; Takahashi et al., 2009). The air-sea CO_2 exchange is a balance between physical and biological processes and its seasonal cycle is characterized by a dominance of CO_2 uptake through the biological carbon pump in summer and a dominance of CO_2 outgassing through upwelling of carbon-rich deep water in winter (e.g., Lenton et al., 2013; Takahashi et al., 2009). The transition from a net CO_2 source to a net CO_2 sink can be explained by the increase in the CO_2 gradient between ocean and atmosphere (through increasing atmospheric CO_2 concentration), that is, by a stronger physical carbon pump (more uptake or less outgassing). The physical carbon pump will continue to strengthen in the future as long as emissions rise but are modulated by variability in atmospheric forcing on decadal time scales (DeVries et al., 2017; Le Quéré et al., 2007; Wetzel et al., 2005). The direction of change is less clear for the biological carbon pump (Bopp et al., 2013; Laufkötter et al., 2015, 2016). Global warming will generally lead to stronger stratification in the upper ocean and less nutrient input from the deep ocean resulting in a decrease of primary

production. In the SO, however, the projected increase in westerly winds might lead to deeper mixed layers regionally and an increase in primary and export production (Hauck et al., 2015; Leung et al., 2015). In the long-term, stronger productivity in the SO might result in nutrient trapping and a decline in global productivity (Moore et al., 2018).

The upper and lower cells of the overturning circulation determine the overturning and north/south exchange in the SO. Both cells are fed by the inflow of North Atlantic Deep Water/Circumpolar Deep Water at mid depth that upwells at the Antarctic Divergence south of the Polar Front. A part of that water (the "upper cell") is then transported northward through surface Ekman transport and subducts as AAIW and SAMW. Another part of the upwelled water (the "lower cell") is transported southward and is exported to depth and out of the SO through Antarctic Bottom Water (AABW) formation. The subduction pathway (upper cell) plays a larger role for nutrient resupply than the AABW pathway (lower cell). This separation has been called the "biogeochemical divide" (Marinov et al., 2006; Primeau et al., 2013).

Along with anthropogenic carbon, the SO exports unutilized macronutrients to the ocean interior via two pathways, namely, subduction of AAIW/SAMW at its northern boundary and AABW formation at the Antarctic shelves. The nutrient export via subduction received a lot of attention, partly motivated to determine the potential for iron fertilization but also due to its potentially important role for lower atmospheric CO_2 during the Last Glacial Maximum (e.g., Petit et al., 1999) and as part of global assessments of nutrient streams (Holzer & Primeau, 2013; Marinov et al., 2006; Palter et al., 2010; Pasquier & Holzer, 2016; Primeau et al., 2013; Sarmiento & Orr, 1991; Sarmiento et al., 2004; Williams et al., 2006).

Using different realizations of ocean circulation and tracer tagging, Palter et al. (2010) suggested that between 33% and 75% of low-latitude productivity is sustained by nutrient export from SAMW, building on the previous work of Sarmiento et al. (2004). Holzer and Primeau (2013) in contrast using a data-assimilation approach, suggested that only 27% of the production in the midlatitude and subpolar North Atlantic would be fuelled by nutrients last utilized in the SO with even lower numbers elsewhere (Holzer & Primeau, 2013). They showed increasing nutrient utilization in the SO resulted in a larger fraction of nutrients last utilized in the SO (up to 45%) but decreased the overall productivity (Holzer & Primeau, 2013). Primeau et al. (2013) further explored this response by both increasing and decreasing nutrient utilization in the SO and found a nonlinear response of productivity outside the SO to perturbations within the SO. This illustrates the state dependence of this response and the nonlinear nature of the link between the SO and the low latitudes.

The efficiencies of the physical and biological carbon pumps in the SO control the dissolved inorganic carbon (DIC) concentration in the mode and intermediate water masses and therefore set the baseline for CO_2 exchange in the low latitudes. Further transformation of the DIC concentration in the SAMW/AAIW will occur, for example, via remineralization during the water mass transport to upwelling regions. The role of the SO on nutrient cycling outside the SO received a lot of attention (Holzer & Primeau, 2013; Palter et al., 2010; Primeau et al., 2013; Sarmiento et al., 2004). However, the impact of SO carbon cycle processes on the global air-sea CO_2 exchange has not been extensively studied. Marinov et al. (2006) investigated the effect of SO nutrient depletion on atmospheric CO_2, that is, to a perturbation from the equilibrium state of Sarmiento et al. (2004) and found that the AABW pathway is more important for sequestering carbon away from the atmosphere.

While all the above previously mentioned studies analyzed the equilibrium transport or the equilibrium response to a perturbation, none of these looked at the transient response to a perturbation. Recently, large interannual variability in high-latitude Southern Hemisphere surface climate (Jones, Gille, et al., 2016) and a large decadal variability of the SO carbon sink (Landschützer et al., 2015; Le Quéré et al., 2007) have been reported. Furthermore, nutrient concentrations show signals of variability or change in multiple regional studies from surface to depth (Ayers & Strutton, 2013; Hoppema et al., 2015; Iida et al., 2013; Panassa et al., 2018; Pardo et al., 2017). Given that mode and intermediate water masses reach the subtropical thermocline on a time scale of a few decades (Jones, Meijers, et al., 2016; Rodgers et al., 2003), it is very likely that these changes may reappear in the low latitudes on a time scale relevant to human anthropogenic CO_2 emissions and emission reduction endeavors (Palter et al., 2010; Pasquier & Holzer, 2016).

In this study, we aim to characterize the time scales of biologically and physically driven air-sea CO_2 flux in the SO, and explore its connection to the air-sea CO_2 exchange and primary and export production outside of the SO. To this end we perform idealized model simulations with an ocean biogeochemical model, which is described in section 2. We perform perturbations that inhibit the biologically and physically driven air-sea

CO_2 exchange in the SO while keeping circulation constant, so that we are able to quantify (i) the sensitivities of large-scale biogeochemistry and carbon cycling to biological productivity and gas exchange over the SO and (ii) the service that the SO provides to us through its active physical and biological carbon pumps. This is the first study that (1) analyzes the transient response to a SO perturbation, that (2) considers perturbations of the gas-exchange in addition to the nutrient utilization, and that (3) applies a primary production module to these questions which is more complex than just translating surface macronutrient utilization to export production.

2. Model and Model Experiments

2.1. MITgcm-REcoM2

The Massachusetts Institute of Technology general circulation model (MITgcm, MITgcm Group, 2017) is coupled to the biogeochemistry and ecosystem model Regulated Ecosystem Model with two phytoplankton classes (REcoM2, Hauck et al., 2013, 2016). The model is configured globally without the Arctic Ocean on a 2° longitude × 0.38–2° latitude grid with the higher resolution around the equator and in the SO. The grid has 30 vertical layers with their thickness increasing from 10 m at the surface to 500 m in the deep ocean. REcoM2 simulates 21 tracers, including DIC and alkalinity for the carbonate system, the macronutrients dissolved inorganic nitrogen (DIN) and silicic acid and the trace metal iron. REcoM2 has two phytoplankton classes, nanophytoplankton (with implicit representation of calcifiers), and diatoms. The intracellular stoichiometry of C:N:Si:Chl pools for diatoms and C:N:$CaCO_3$:Chl pools for nanophytoplankton is allowed to respond dynamically to environmental conditions (Geider et al., 1998). The intracellular iron pool is a function of the intracellular nitrogen concentration (fixed Fe:N) as iron is physiologically linked to enzyme formation, especially to the photosynthetic electron transport chain (Behrenfeld & Milligan, 2013; Raven, 1988). Dead organic matter is transferred to one detritus class by aggregation and grazing by one zooplankton class. The sinking and advection of detritus is represented explicitly. Detritus sinks with a sinking velocity that increases with depth (Kriest & Oschlies, 2008, from 20 m/day at the surface to 170 m/day at 5,300 m depth). This setup is identical to Hauck et al. (2016) except for two parameter settings, namely, iron solubility from dust input is now set to 1% and nanophytoplankton chlorophyll degradation rate is set to 0.1 d^{-1}.

2.2. Model Forcing and Spin-Up

The model was forced by the atmospheric forcing fields from the 6-hourly Japanese 55-year Reanalysis (JRA-55, Kobayashi et al., 2015). We spun up the model by repeating the JRA-cycle for 1958–2015 (58 years) twice. The third JRA cycle was run until the year 2005, so that the total spin-up was 164 years. The model DIC field was initiated with preindustrial DIC from GLODAP (Key et al., 2004), and the model was forced with rising atmospheric CO_2. In terms of atmospheric CO_2 concentration, we treated these 164 years of spin-up as following the historical atmospheric CO_2 concentration from 1842 to 2005 provided by the Global Carbon Budget (Le Quéré et al., 2018). This data set averaged the atmospheric CO_2 concentration from the Mauna Loa and South Pole stations from 1958 onward (Dlugokencky & Tans, 2016; Keeling et al., 1976) and used a cubic spline fit to ice core data before 1958 (Joos & Spahni, 2008).

2.3. Model Experiments

In order to track the northward propagation of carbon and nutrient signals caused by the physically and biologically driven carbon pumps in the SO, we performed six idealized model simulations for 200 years with constant atmospheric forcing fields. We focused on the 200-year time scale as more than 70% of the perturbed SAMW/AAIW nutrient signal will have reached the tropics and be upwelled within 200 years (Rodgers et al., 2003) and because this is the relevant time scale to the transient response. The first set of model experiments (CTRL, NOBIO, and NOBIOGASEX, see Table 1) were started after the year 2005 by keeping atmospheric forcing fields and CO_2 concentration constant at their 2005 states (atmospheric CO_2 concentration of 378 ppm) for the following 200 years.

The first simulation is the control simulation (CTRL), which is the standard setup of the model. In the second simulation (NOBIO) we switched off primary production south of 40°S. In the third simulation (NOBIOGASEX), we switched off primary production and gas-exchange south of 40°S. The differences in CO_2 air-sea exchange, nutrients, DIC, and primary and export production between the CTRL and the NOBIO simulations ($contrib_{bio}$ = CTRL − NOBIO) are caused by the biological carbon pump in the SO. The air-sea CO_2 exchange that still occurs in the NOBIO simulation is fully driven by abiotic processes, for example, upwelling of carbon-rich deep water or temperature effects on CO_2 solubility. This air-sea CO_2 exchange was suppressed in the NOBIO-

Table 1
Model Experiments

Simulation	Perturbation	Length	Forcing	Atm CO_2
CTRL	none	200 years	2005	378 ppm
NOBIO	No NPP south of 40°S	200 years	2005	378 ppm
NOBIOGASEX	No NPP + no gas-exchange south of 40°S	200 years	2005	378 ppm
CTRL-diseq	none	200 years	2005	increasing with 1.98 ppm/year
NOBIO-diseq	No NPP south of 40°S	200 years	2005	increasing with 1.98 ppm/year
NOBIOGASEX-diseq	No NPP + no gas-exchange south of 40°S	200 years	2005	increasing with 1.98 ppm/year

Note. See text for detailed description.

GASEX simulation. Therefore, we consider the differences between the NOBIO and NOBIOGASEX simulations ($contrib_{phys}$ = NOBIO − NOBIOGASEX) to be caused by the physically driven CO_2 uptake in the SO.

In a second set of experiments ("-diseq" in Table 1), we tested the effect of atmospheric CO_2 forcing by increasing atmospheric CO_2 with the average rate of increase between 2000 and 2010 (1.98 ppm/year, 773 ppm at the end of the experiment). We chose this atmospheric CO_2 forcing to mimic the current atmospheric CO_2 increase rather than a faster increase in the future.

We focus on the first set of experiments with constant atmospheric CO_2 throughout this study. The effect of increasing atmospheric CO_2 will be discussed in sections 4.3.1 and 4.4.

3. Unperturbed Model State

The model was evaluated in previous publications (Hauck et al., 2013, 2016). In the year 2005, just before the start of the perturbation experiments, the global ocean CO_2 uptake amounts to 2.0 PgC year^{-1}, which is in the center of the range of modelled values for 2005 (Le Quéré et al., 2018). The SO south of 40°S contributes 1.0 PgC year^{-1} to the total ocean carbon sink, which is at the higher end of the observational range (Landschützer et al., 2015; Lenton et al., 2013). The model reasonably simulates the seasonal cycle of CO_2 uptake in the SO (Hauck & Völker, 2015). Global net primary production (NPP) amounts to 36 PgC year^{-1} in model year 2005 with a contribution of 6.8 PgC year^{-1} from the SO. This leads to an export production of 9.4 PgC year^{-1} globally and of 2.9 PgC year^{-1} in the SO. We estimate the SAMW/AAIW export out of the SO by calculating the transport across 31°S in the neutral density range 26.8–27.3 (Downes et al., 2017). The resulting SAMW/AAIW transport of 8 Sv is consistent with the 8 Sv estimated across 30°S by Talley (2013).

4. Results and Discussion

Switching off primary production in the SO leads to a nutrient and carbon anomaly that is transported northward. This signal ($contrib_{bio}$) allows us to quantify the effect that biological processes in the SO, when active, have on the global nutrient distribution (section 4.2) as well as on the DIC distribution and air-sea CO_2 exchange (4.3). All air-sea CO_2 exchange in NOBIO is driven by abiotic ("physical") processes, for example, circulation or temperature effects on air-sea CO_2 exchange. The difference between NOBIO and the simulation NOBIOGASEX, where all gas-exchange is inhibited, therefore allows us to quantify the effect that physically driven air-sea CO_2 exchange in the SO has on the global DIC distribution and air-sea CO_2 exchange outside of the SO ($contrib_{phys}$).

4.1. Time Scale of Re-Emergence

The perturbation signal from the SO emerges after 15 years in the equatorial Atlantic (5°S to 5°N) and after approximately 50 years in the equatorial Pacific as illustrated by the time-series of export production (Figure 1). This is broadly consistent with the estimate of a minimum travel time of 28 years and a median travel time of 92 years for SAMW from its formation region to the Equatorial Undercurrent in the Pacific (Rodgers et al., 2003). The major reason for the difference between the Lagrangian study of Rodgers et al. (2003) and the present Eulerian study is the neglect of eddy diffusivity in the Lagrangian study. Shah et al. (2017) showed the importance of including stochastic terms in Lagrangian models to account for transport by eddies. Our time scales are also somewhat shorter because our experiment includes perturbed carbon and nutrient concentrations in the surface transport and not only mode and intermediate water masses. In contrast, Rodgers et al. (2003)

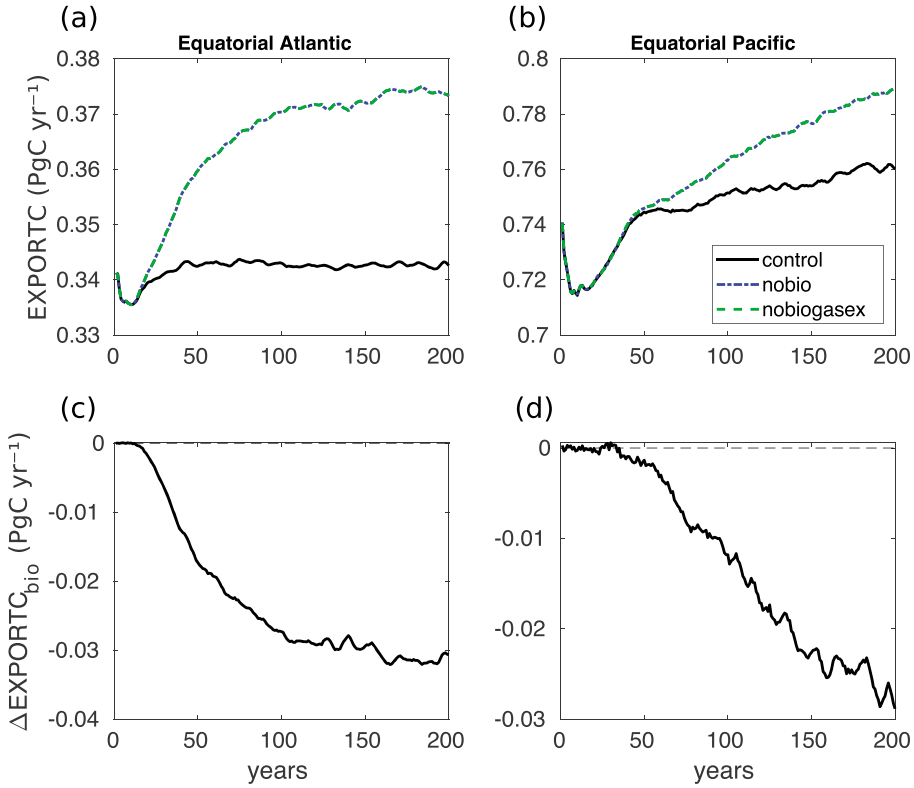

Figure 1. Time series of carbon export (PgC year^{-1}) across 100 m depth in two latitudinal bands (±5°) around the equator, for (a) the Atlantic and (b) the Pacific. Also shown are the differences (ΔEXPORTC$_{bio}$) between the CTRL and the NOBIO simulation (CTRL − NOBIO) in the (c) equatorial Atlantic and (d) equatorial Pacific.

released passive particles in a Lagrangian trajectory analysis and applied also a stricter definition of the equatorial upwelling region only in the Pacific. The estimated time of re-emergence is also in line with the estimate that 50% of each mode water tracer reaches the subtropical thermocline in 50 years (Jones, Meijers, et al., 2016).

4.2. The Fate of Nutrients Exported Out of the SO

In the following, we discuss the contribution of active SO biology on nutrient distribution and NPP that we define as contrib$_{bio}$ = CTRL − NOBIO. On the time scale of 200 years considered here, active biological processes in the SO lead to a gradient in nutrient distribution by reducing macronutrient and micronutrient concentration in the surface of the SO and in the exported intermediate water masses (Figure 2). The signal of reduced DIN concentration reaches down to approximately 1,500 m and up to 20°N in the Pacific Ocean, whereas the signal spreads down to below 4,000 m and reaches the northern limit of our model setup at 80°N in the Atlantic Ocean (Figures 2a and 2b). A stronger DIN response to active SO biology occurs in the Atlantic than in the Pacific. This was anticipated in response to the stronger overturning in the Atlantic and is consistent with previous studies (Holzer & Primeau, 2013; Primeau et al., 2013; Sarmiento et al., 2004). The weak signal in the Pacific is also supported by De Lavergne et al. (2017) who described a shadow zone of the overturning in the depth range of 1 to 2.5 km in the Pacific and Indian Oceans where there is no AABW return flow. In the Atlantic, the northern surface source of deep water disrupt the middepth zone (De Lavergne et al., 2017), which is consistent with the negative DIN anomaly in the deep North Atlantic.

The sinking of particles and remineralization with active SO biological pump increases the DIN concentrations in the subsurface of the SO, which might be amplified by nutrient trapping. This signal is transported out of the SO via the AABW pathway to the Atlantic and Pacific Ocean basins. Outside of the SO, active SO biology produces a positive DIN signal below approximately 4,000 m in the Atlantic and below approximately 3,000 m in the Pacific Ocean in our model. Consistent with Holzer and Primeau (2013) and Primeau et al. (2013), we do not only perturb the SAMW/AAIW source region but the SO surface south of 40°S. Consequently, higher

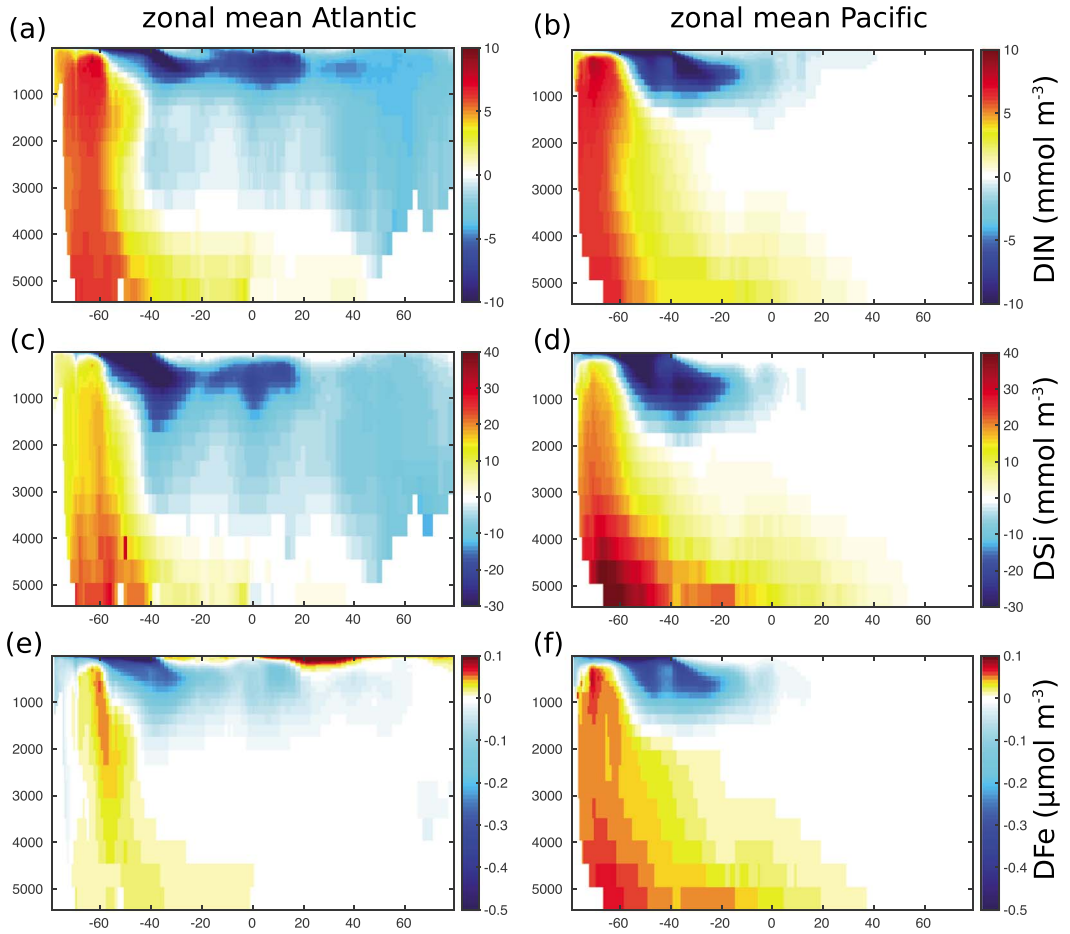

Figure 2. Effect of active primary production (CTRL − NOBIO) in the Southern Ocean on zonal mean nutrient distributions in the (a, c, and e) Atlantic and (b, d, and f) Pacific Ocean. Shown are zonal means averaged over the last 5 years of the 200-year perturbation simulations of (a–b) dissolved inorganic nitrogen, (c–d) dissolved silicic acid, and (e–f) dissolved iron. Note different scales for different nutrients.

nutrient concentrations will also follow other than just the SAMW/AAIW pathways (surface transport, lower cell, and southward return flow; see also Holzer & Primeau, 2013).

The maximum positive anomaly of silicic acid lies below 4,000 m (Figures 2c and 2d), which is considerably deeper than the maximum positive anomaly of DIN which is located at about 500 m within the SO (Atlantic and Pacific sectors). This mirrors the fact that the opal dissolution rate is slower than the degradation rate of particulate organic nitrogen to dissolved organic nitrogen and the remineralization rate of dissolved organic nitrogen to DIN. Active SO biology has a similar impact on dissolved iron, with the maximum of the positive signal at about 500 m in the Atlantic and the Pacific (Figures 2e and 2f). In the Pacific, a secondary maximum is found close to the seafloor. Maybe counterintuitively, activating the biological carbon pump in the SO is responsible for a positive anomaly of iron in the surface of the Atlantic Ocean. We explain this by the strong iron input by dust in the Atlantic (Mahowald et al., 2005) and the resulting nitrate limitation. The utilization of DIN in the SO, even if not complete, reduces the amount of DIN available in the surface Atlantic leaving more iron unutilized. Our model includes DIN as the only macronutrient and does not consider nitrogen fixation. In the real world, nitrogen fixation would compensate the external supply of DIN. We hypothesize that phosphate limitation might then lead to the same effect on iron, but this would have to be tested in a model carrying phosphate.

The NPP in the SO amounts to 7.0 PgC year^{-1} in the control simulation (Figure 3a). Switching off this primary production leads to an augmentation of NPP north of 40°S by 3.0 PgC year^{-1} at the end of the 200-year simulation (Figure 3b). This is an increase of 10% relative to the unperturbed NPP of 29.8 PgC year^{-1} in the control simulation. By turning off active biology in the SO, the decrease in NPP within the SO (7.0 PgC year^{-1}) is only

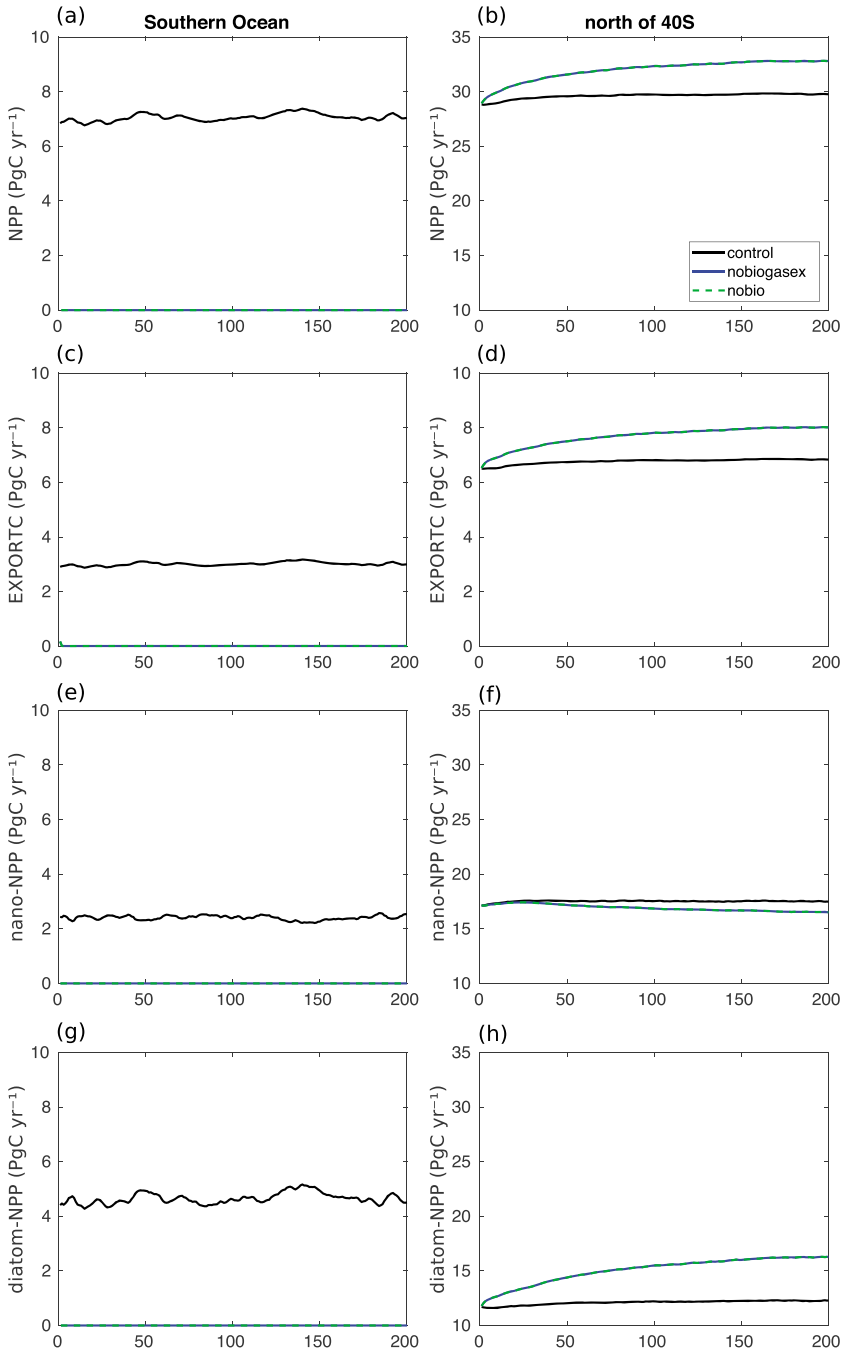

Figure 3. Time series of (a and b) vertically integrated net primary production, (c and d) export production across 100 m, (e and f) nanophytplankton NPP, (g and h) diatom NPP in the (left) Southern Ocean and (right) north of 40°S. Note the different scales within and out of the Southern Ocean and that the scale for export differs from NPP scales north of 40°S.

offset by 3.0 PgC year^{-1} outside the SO (43%). Hence, only 43% of the SO NPP would be compensated outside of the SO on a 200-year time scale. Export production at 100 m (EP) displays a similar response (Figures 3c and 3d). The SO export production with active biology is 3.0 PgC year^{-1}. By switching off SO NPP, export north of 40°S increases by 1.2 PgC year^{-1} after 200 years (17% increase). Only 39% of suppressed SO export is compensated outside the SO.

Diatoms and nanophytoplankton contribute differently to the 43% compensation of NPP outside the SO (Figures 3e–3h). Diatom NPP is nearly completely compensated outside the SO. Switching off 4.5 PgC year^{-1}

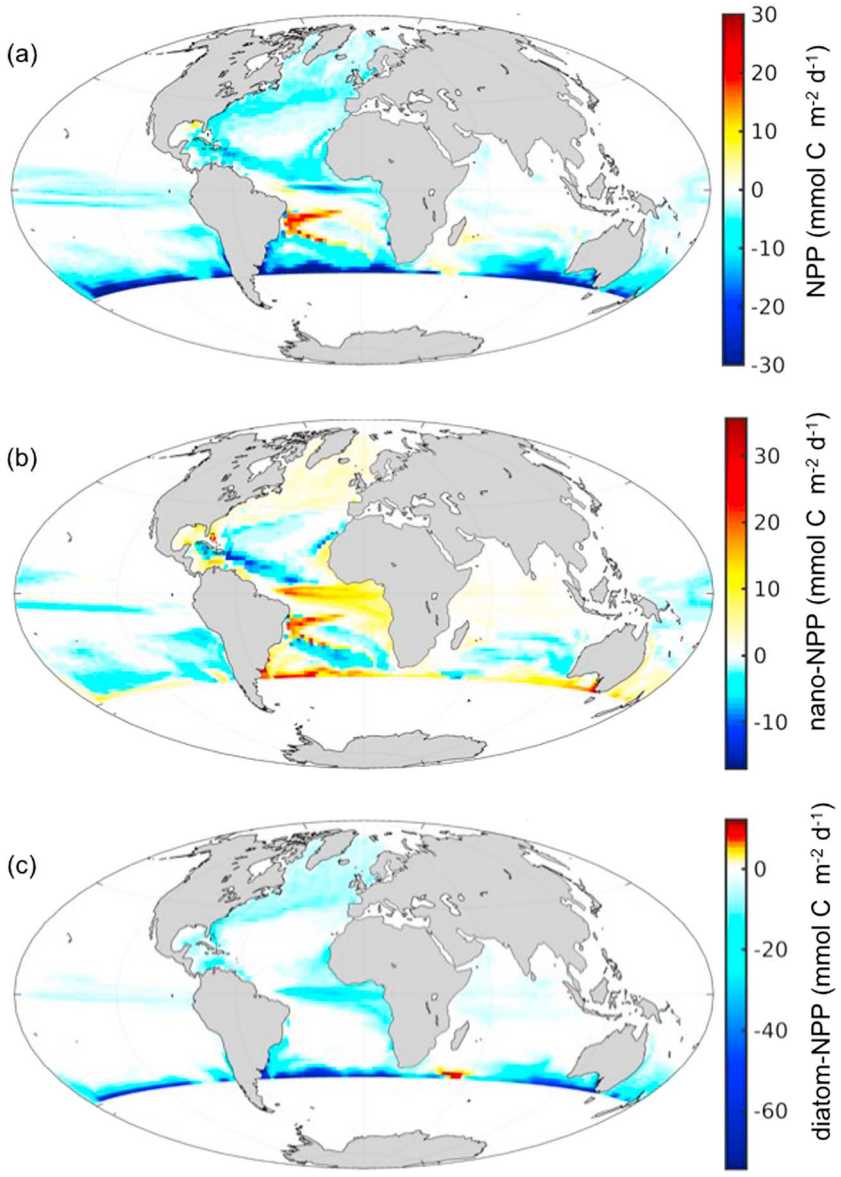

Figure 4. Effect of active primary production (CTRL-NOBIO) in the Southern Ocean on vertically integrated net primary production (NPP) outside the Southern Ocean. Shown are (a) total NPP, (b) nanophytoplankton NPP, (c) diatom NPP averaged over the last 5 years of the 200-year perturbation simulations. All units are mmol C m^{-2} d^{-1}.

diatom NPP in the SO in CTRL is compensated by 3.9 PgC $year^{-1}$ diatom NPP increase in NOBIO outside the SO (Figures 3e and 3f). This corresponds to a 32% increase of diatom NPP outside the SO and a 87% compensation of SO diatom NPP. In contrast, switching off active biology in the SO leads to a reduction of nanophytoplankton NPP both inside and outside of the SO (Figures 3g and 3h). The suppression of 2.5 PgC $year^{-1}$ nanophytoplankton NPP in the SO is associated with a further 1.0 PgC $year^{-1}$ reduction north of 40°S in NOBIO relative to CTRL. This translates to a 6% decrease of nanophytoplankton NPP outside the SO and a reinforcement rather than a compensation of SO nanophytoplankton NPP.

The spatial patterns of active SO biology effects ($contrib_{bio}$) on total, diatom and nanophytoplankton NPP are shown in Figure 4. Total NPP outside the SO is negatively affected by active SO biology with the strongest signal in the Atlantic and an exception in the subtropical gyre in the South Atlantic (Figure 4a). The stronger Atlantic response might be a time scale dependent feature but may reflect stronger connectivity between SO mode and intermediate waters with the North Atlantic than with the North Pacific (Holzer & Primeau, 2013; Primeau et al., 2013; Sarmiento et al., 2004). Diatom productivity outside the SO is almost everywhere

negatively affected by active SO biology with the strongest effects at the boundary to the SO, in the subpolar North Atlantic and equatorial Atlantic (Figure 4c). Nanophytoplankton shows a pattern of being positively affected where diatom NPP is negatively affected and being negatively affected where there is no effect on diatom NPP (Figure 4b). In summary, nanophytoplankton NPP is positively affected by active SO biology as also shown above with the decrease of nanophytoplankton NPP in NOBIO (Figures 3g and 3h).

We explain these effects of active SO biology on diatom and nanophytoplankton NPP outside the SO as follows. Biological production in the SO binds silicic acid that is not available for diatom productivity outside of the SO. As a result, active SO biology in the SO has a negative impact on diatom productivity and a positive effect on nanophytoplankton productivity outside the SO (Figure 4). Switching off biology in the SO leads to an increase in diatom productivity outside the SO due to increased silicic acid availability, which can then outcompete nanophytoplankton in many regions. The export of nutrients out of the SO therefore affects not only the total amount of NPP outside the SO but also the phytoplankton community composition. This mechanism was described as "silica leakage," and it was hypothesized to contribute to an atmospheric CO_2 drawdown during glacial times by weakening the carbonate pump outside the SO (Brzezinski et al., 2002; Matsumoto et al., 2002).

The mean 17% increase of EP north of 40°S without active SO biology is in the same range as the unperturbed (ca. 5–25% SO-sustained export production outside the SO) and the perturbed estimate (ca. 10–45%) by Holzer and Primeau (2013) in their data-assimilated phosphorous cycle model. Global export production is controlled mainly by the nutrient transport by the upper cell (Marinov et al., 2006); as the upper cell will be close to equilibrium after 200 years, we expect this result not to differ qualitatively from an equilibrium response. The increase of production in the rest of the world in response to a SO production shutdown can be explained by a higher fraction of unutilized nutrients and might be reinforced by relieving nutrient trapping (Primeau et al., 2013), that is, by reduced sinking of particles to southward flowing waters at middepth that short circuit the surface northward flow. However, both our and the estimates of Holzer and Primeau (2013) and Primeau et al. (2013) seem to be at odds with the statement that SO nutrient supply accounts for 75% of biological production north of 30°S by Sarmiento et al. (2004). These differences reflect differences in the mean ocean state and the nature of the simulations, specifically we perform the experiment with the reverse sign as compared to Sarmiento et al. (2004). Primeau et al. (2013) and Holzer and Primeau (2013) illustrated that the system's response in and outside of the SO to a nutrient perturbation is state dependent and not linear and a larger effect is expected from forcing the model to complete nutrient utilization than to zero nutrient utilization, even if the magnitudes of SO surface nutrient change is similar (Sarmiento: 100% change; our experiment: DIN 75%, silicic acid 255%, and iron 340%).

4.3. The Fate of Carbon Taken up in the SO

As in section 4.2, we refer to the contribution of SO biological production, when active, as $\text{contrib}_{\text{bio}} = \text{CTRL} - \text{NOBIO}$ and to the contribution of the physical carbon pump as $\text{contrib}_{\text{phys}} = \text{NOBIO} - \text{NOBIOGASEX}$.

4.3.1. Air-Sea CO_2 Flux

The global CO_2 uptake in the CTRL simulation declines over the 200-year simulation, because in our simulation we keep the atmospheric CO_2 concentration constant (Figure 5). In CTRL, the CO_2 flux amounts to −0.52 PgC year^{-1} in the SO at the end of the 200-year simulation (Figure 5a). The air-sea CO_2 exchange in the SO can be separated into $\text{contrib}_{\text{bio}}$ and $\text{contrib}_{\text{phys}}$. Active SO biology leads to CO_2 uptake ($\text{contrib}_{bio} = -1.14$ PgC year^{-1}, Figure 5c), whereas abiotic processes lead to CO_2 outgassing ($\text{contrib}_{phys} = +0.62$ PgC year^{-1}, Figure 5e).

There is a mean outgassing flux by 0.2 PgC year^{-1} at the end of the 200-year simulation outside the SO (Figure 5b). Active SO biology leads to a tendency to outgas of 0.57 PgC year^{-1} (contrib_{bio}, Figure 5d). However, the SO physical carbon pump leads to a tendency for CO_2 uptake of nearly the same amount outside the SO (−0.55 PgC year^{-1}, Figure 5f). In total, the SO carbon pumps trigger a net outgassing of only 0.02 PgC year^{-1} outside the SO (Figure 5h). These large and opposing tendencies of CO_2 flux outside the SO by SO physics and biology suggest that stronger changes in one of the SO carbon pumps, without a change in the other, can trigger a strong response in the global air-sea CO_2 exchange. For example, the strong variability in the SO physical carbon pump (here more outgassing, DeVries et al., 2017; Le Quéré et al., 2007; Wetzel et al., 2005) with an incomplete compensation through the biological carbon pump (DeVries et al., 2017; Dufour et al., 2013; Hauck et al., 2013) might trigger a response of larger CO_2 uptake in areas remote from the SO. Similarly, a long-term increase in SO productivity (Moore et al., 2018) without equivalent changes in the physical pump would lead to less CO_2 uptake/more outgassing outside the SO.

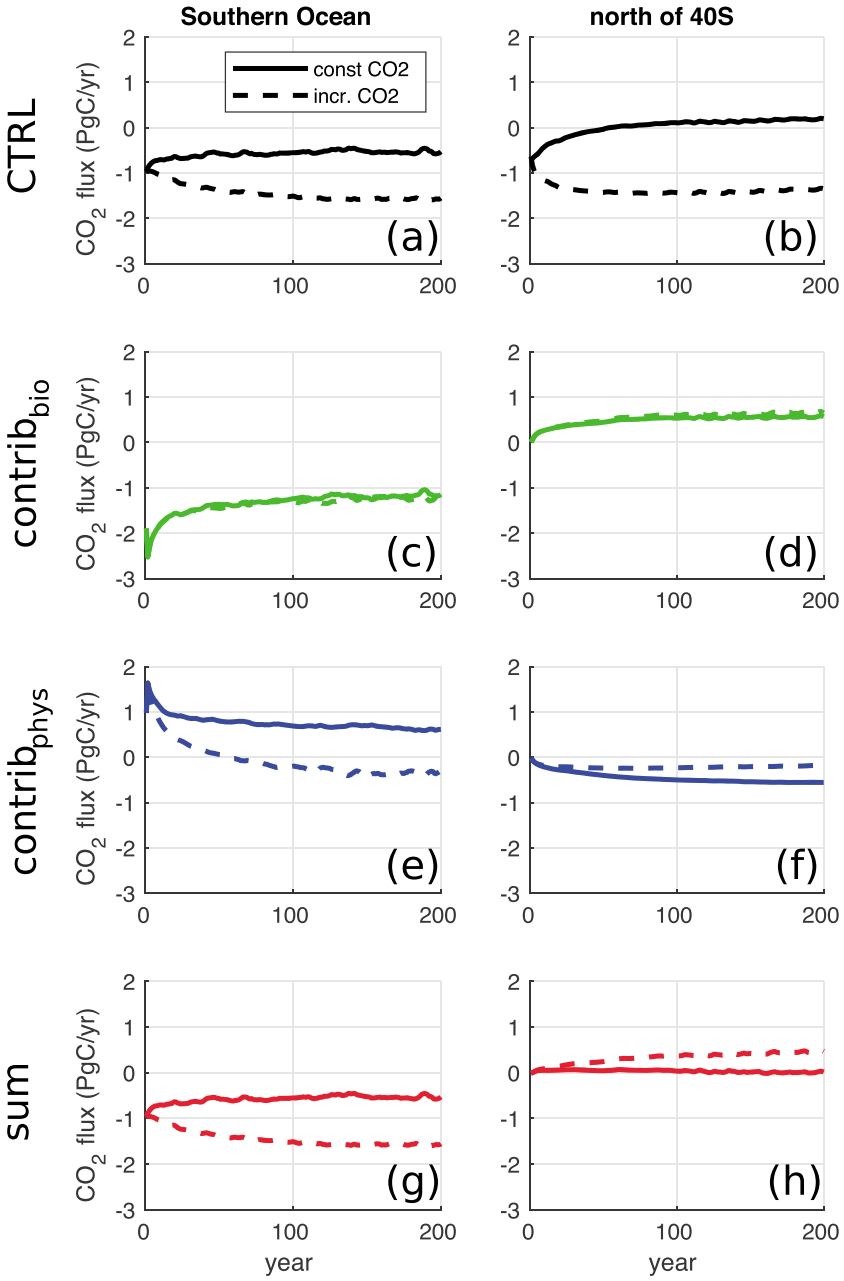

Figure 5. Unperturbed air-sea CO_2 exchange (CTRL, a and b) and anomalies thereof due to perturbations (c–h) in the (left) Southern Ocean and (right) north of 40°S. Lines show standard simulations with constant atmospheric CO_2, dashed lines show disequilibrium simulations with increasing atmospheric CO_2 concentration. Shown are (c–d) SO-biology contribution to air-sea CO_2 exchange (CTRL-NOBIO), (e–f) SO-physics contribution to air-sea CO_2 exchange (NOBIO-NOBIOGASEX), (g–h) sum of SO-biology and SO-physics contribution to air-sea CO_2 exchange. Positive CO_2 flux indicates (tendency to) outgassing, negative CO_2 flux indicates (tendency to) CO_2 uptake.

In the set of simulations with increasing atmospheric CO_2 concentration, there is by design a larger flux of CO_2 into the ocean within and outside of the SO (Figure 5, dashed lines). There is hardly any difference in the effect of active SO biology on global CO_2 uptake (Figures 5c and 5d). At the beginning of the simulation, abiotic processes in the SO lead to CO_2 outgassing and a negative DIC anomaly in the exported AAIW/SAMW. During the simulation, the sign of the contrib$_{phys}$ changes and after 50 years abiotic processes start leading to CO_2 uptake in the SO. This is merely caused by the increasing atmospheric CO_2 concentration. The negative DIC anomaly in the AAIW/SAMW persists for longer, particularly in the Pacific (Figure S1 in the supporting information). At the end of the 200-year experiment, abiotic processes in the SO lead to an uptake of CO_2

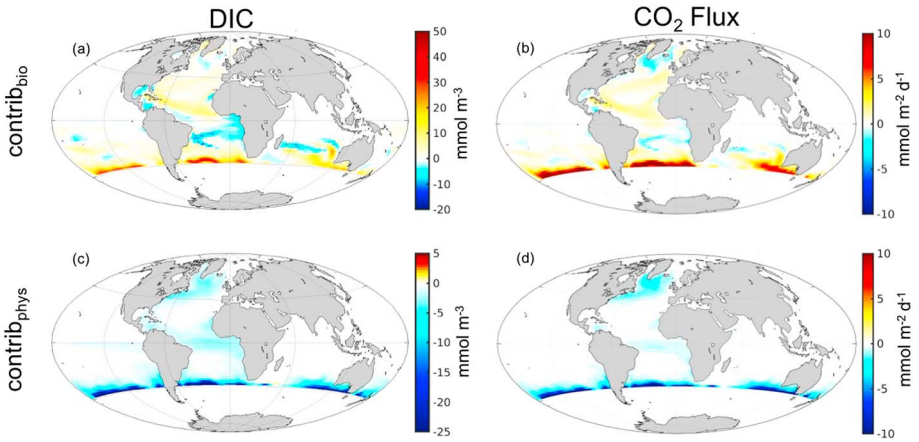

Figure 6. Surface DIC (a and c) and CO_2 flux (b and d) anomalies caused by Southern Ocean processes, (a and b) biological carbon pump (CTRL − NOBIO) and (c and d) physical carbon pump (NOBIO − NOBIOGASEX). Shown are the averages over the last 5 years of the 200-year perturbation simulations. Positive CO_2 flux anomalies indicate (tendency to) outgassing, negative CO_2 flux anomalies indicate (tendency to) CO_2 uptake.

($contrib_{phys} = -0.55$ PgC year^{-1}) in the SO. At the same time, the lagged negative DIC anomaly signal resulting from abiotically driven SO CO_2 outgassing in the beginning of the simulation, still leads to CO_2 uptake outside of the SO ($contrib_{phys} = -0.18$ PgC year^{-1}). In total, the biological and physical carbon pumps in the SO lead to outgassing of 0.47 PgC year^{-1} in the disequilibrium simulation. Note that this number is a snapshot and is further away from equilibrium than in the simulation with constant atmospheric CO_2 due to the change of sign of abiotically driven air-sea CO_2 exchange in the SO. The derived role of the SO physical carbon pump for the global carbon cycle depends critically on the choice of prescribed atmospheric CO_2 concentration and the timing of reversal of air-sea CO_2 flux in the SO which shapes the history of DIC in the AAIW/SAMW.

4.3.2. Patterns of Surface Changes

The active SO "physical" carbon pump leads to negative surface DIC anomalies outside the SO, which are strongest in the Atlantic Ocean (Figure 6c). It further leads to negative CO_2 flux anomalies (more uptake) in the North Atlantic, in the equatorial Atlantic and in the Atlantic Eastern Boundary Upwelling Systems (Figure 6d), apart from negative anomalies directly adjacent to our arbitrary boundary at 40°S. The latter is an artefact of waters crossing the boundary at 40°S, north of which gas exchange is allowed.

In contrast, active "biological processes" lead to a positive surface DIC and CO_2 flux anomaly (more outgassing or less uptake by the ocean) in the central and subtropical North Atlantic and at the boundary to the SO (Figures 6a and 6b). Notable exceptions are the southern Atlantic subtropical gyre and the North Atlantic subpolar gyre with negative surface DIC and CO_2 flux anomalies (Figures 6a and 6b). We consider two possible explanations for the positive DIC anomalies. Either upwelling of remineralized carbon leads to the increase in surface DIC concentration or the export of nutrient-depleted surface water reduces NPP and thereby causes positive DIC anomalies. We reject the first hypothesis (upwelling of remineralized carbon) as this DIC signal would have to be apparent in the subsurface DIC anomalies, which it is not (Figure 7). The second hypothesis (reduced NPP) is supported by our analysis of NPP which shows negative anomalies related to biological production in the SO. The "negative" surface DIC and CO_2 flux anomalies (more CO_2 uptake) in the north Atlantic subpolar gyre can only be explained by upwelling of DIC-depleted water. NPP anomalies go in the opposite direction (less NPP) and cannot contribute to enhanced North Atlantic CO_2 uptake caused by the active biological carbon pump in the SO. The negative DIC anomaly reaching up to the surface is also evident from Figure 7. The active SO biological carbon pump leads to a positive anomaly in nanophytoplankton productivity (Figure 4) and calcification (not shown) in the subpolar North Atlantic. The latter leads to a slight reduction of alkalinity (by less than 3 mmol/m^3) at the end of the simulation, which would rather lead to more outgassing than to stronger uptake and can therefore not explain the CO_2 flux anomaly in the subpolar North Atlantic. The negative surface DIC and CO_2 flux anomalies in the south Atlantic seem to be sustained by a combination of upwelling of low-DIC anomalies in the Benguela upwelling system (Figures 7 and 6) and a positive NPP anomaly caused by nanophytoplankton in the western south Atlantic (Figures 4).

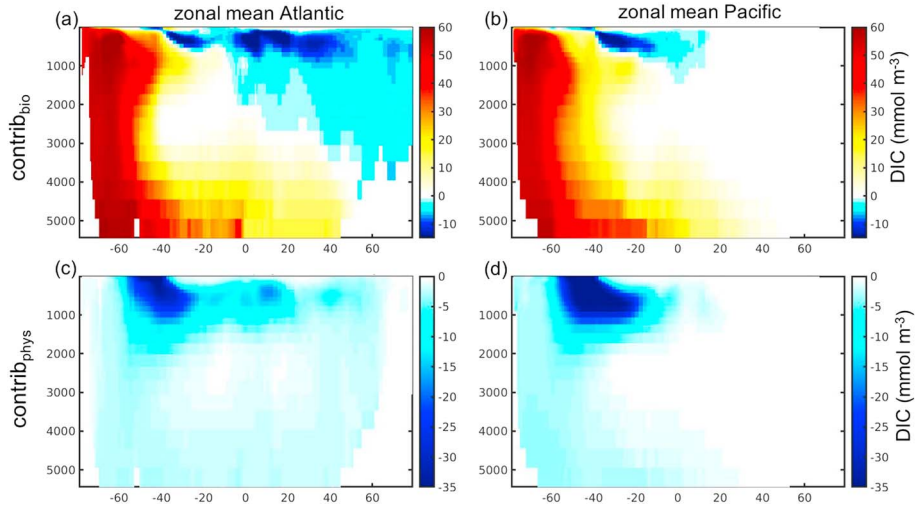

Figure 7. Contribution of Southern Ocean (a–b) biological carbon pump (CTRL − NOBIO) and (c–d) physical carbon pump (NOBIO − NOBIOGASEX) to zonal mean DIC distribution in the (a and c) Atlantic and (b and d) Pacific. Shown are the averages over the last 5 years of the 200-year perturbation simulations. Note the different scales for biological and physical contributions.

4.3.3. DIC Inventory

An active SO biological carbon pump transports carbon into the deep ocean. The biologically driven inventory of DIC in the SO has increased by 125 PgC after 200 years of experiment in the full water column south of 40°S and by 42 PgC below 3,000 m (Figures 7a and 7b). The physical carbon pump, in contrast, leads to a reduction of the DIC inventory by 26 PgC in the full water column of the SO and by 3 PgC below 3,000 m due to strong outgassing in the south at constant atmospheric CO_2 concentration of 378 ppm (Figures 7c and 7d). This outgassing is related to the upwelling of carbon-rich deep water in the SO, which brings water to the surface, which has a higher pCO_2 than the atmosphere. In accord with the solubility pump, this leads to outgassing of CO_2 to the atmosphere without biology drawing down this carbon in summer. In the experimental setup with increasing atmospheric CO_2 concentration, the SO physical carbon pump turns from outgassing to uptake when the atmospheric pCO_2 becomes larger than the pCO_2 in SO upwelled water. In this simulation which is characterized by abiotically driven outgassing in the beginning and abiotically driven uptake after about 50 years, the DIC inventories in the SO at the end of the experiment amount to 122 PgC (biologically driven, SO), 41 PgC (biologically driven, SO below 3,000 m), 52 PgC (abiotically driven, SO), and 16 PgC (abiotically driven, SO below 3,000 m).

4.4. Implications for Carbon Uptake, Transport and Storage

We defined a term compensation factor F_C of air-sea CO_2 exchange through the SO biological carbon pump as

$$F_{C\,bio} = \frac{-\text{contrib}_{\text{bio, north of 40°S}}}{\text{contrib}_{\text{bio, south of 40°S}}} \quad (1)$$

and similarly a term for the compensation of air-sea CO_2 exchange through the SO physical carbon pump as

$$F_{C\,phys} = \frac{-\text{contrib}_{\text{phys, north of 40°S}}}{\text{contrib}_{\text{phys, south of 40°S}}} \quad (2)$$

that is, F_C is 0 if all air-sea CO_2 flux through either of the pumps in the SO does not lead to a change of CO_2 flux outside of the SO, and it is one if all of the CO_2 flux is compensated by a flux of the same magnitude but opposite sign north of 40°S. The same metric can be applied for NPP and a negative F_C can occur if a change in the SO triggers a change outside the SO of the same sign (as for nanophytoplankton NPP).

A larger proportion of the physical signal re-emerges earlier as compared to the biological signal ("nutrient trapping," here "carbon trapping"). As a result, 90% of the instantaneous air-sea CO_2 flux that occurs through the physical pump in the SO is balanced elsewhere after 200 years (Figure 8a). The biological carbon pump sequesters carbon for longer as only 50% of the instantaneous air-sea CO_2 flux in the SO is compensated elsewhere at the end of the experiment (Figure 8a). This number is very close to the 43% compensation of

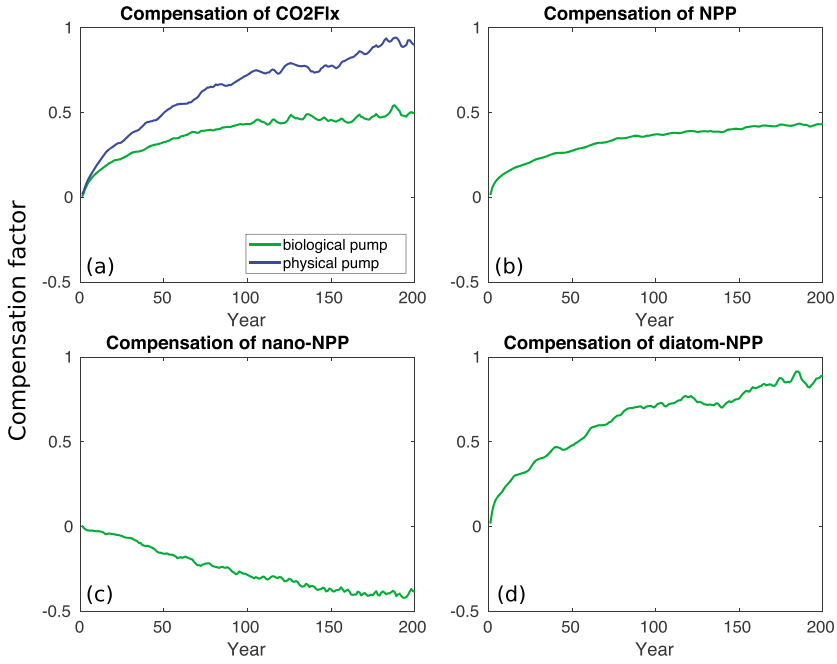

Figure 8. Compensation factor F_C for Southern Ocean (a) CO_2 flux, (b) total net primary production, (c) nanophytoplankton net primary production, and (d) diatom net primary production outside of the Southern Ocean. The compensation factor (see text) is defined to be one if a change (green: $contrib_{bio}$ = CTRL − NOBIO, or blue: $contrib_{phys}$ = NOBIO − NOBIOGASEX) in the Southern Ocean is completely balanced by a change of reverse sign outside the Southern Ocean. The compensation factor is defined to be zero if there is no change outside of the Southern Ocean associated with a change in the Southern Ocean. The compensation factor is negative if a change in the Southern Ocean leads to a change of the same sign outside the Southern Ocean. After 200 years, 50% of biologically driven air-sea exchange (uptake) and 90% of physically driven air-sea exchange (outgassing) in the Southern Ocean are balanced by air-sea exchange with reverse sign north of 40°S.

NPP (Figure 8b). The latter is the result of the 90% compensation of diatom production and the negative compensation factor of nanophytoplankton production (Figures 8c and 8d). We therefore consider that two factors contribute to the longer carbon sequestration time for biologically driven carbon uptake (Figure 9).

First, the incomplete compensation of biologically driven CO_2 flux in the upper cell is driven by the incomplete compensation of NPP, which is caused by feedbacks in phytoplankton community composition. Second, the carbon anomalies caused by an active biological carbon pump are twofold: a negative DIC anomaly spreads from the surface via the upper cell, whereas a positive anomaly spreads via the lower cell. The physically induced carbon anomalies occur mostly in the upper cell in our experiments (Figure 7). The sinking and remineralization of organic material lead to the gradient of negative DIC anomalies in the upper cell and positive DIC anomalies in the lower cell. On the time scales considered here, this sustains the incomplete compensation of biologically driven air-sea CO_2 flux and therefore the longer sequestration time scales for the biological carbon pump. In summary (Figure 9), active SO biology leads to CO_2 flux into the ocean in the SO, to DIC increase at depth and DIC and nutrient reduction in the exported upper cell water. The effect of reduced NPP outside the SO dominates over the effect of reduced DIC and leads to positive air-sea CO_2 flux anomalies (more outgassing or less uptake). An exception to that is the subpolar North Atlantic where the effect of reduced DIC dominates. Outgassing in the SO leads to reduced DIC content in the exported upper cell water, which can then take up carbon outside the SO.

While the physical carbon pump to date leads to outgassing in the SO, this implies that 90% of the CO_2 released to the atmosphere would be back in the ocean somewhere else after 200 years. The biological carbon pump in the SO leads to CO_2 uptake and 50% of that CO_2 is still in the ocean after 200 years. While potential future changes in the SO physical carbon pump will be compensated within 200 years, potential future changes in the SO biological carbon pump (e.g., Moore et al., 2018) might lead to significant global carbon feedbacks. This is supported by the conclusion of DeVries et al. (2012) that the SO might dominate the response of the biological carbon pump to potential future export changes using a different methodological

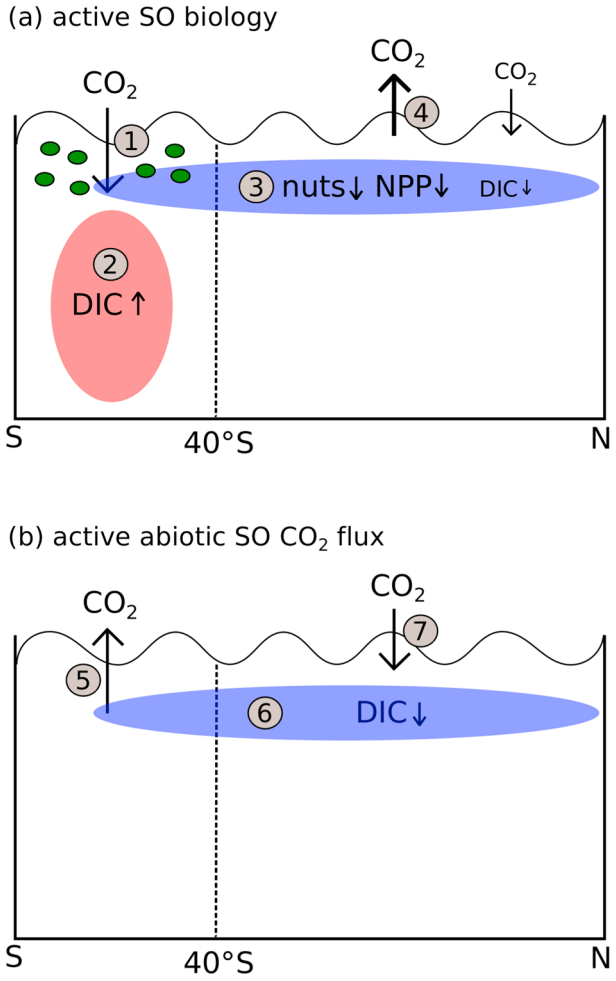

Figure 9. Sketch to illustrate the effects of (a) active Southern Ocean biology and (b) active Southern Ocean abiotic CO_2 flux at constant atmospheric CO_2 on net primary production and CO_2 flux outside of the Southern Ocean. (a) Active Southern Ocean biology leads to (1) CO_2 flux into the ocean in the SO, to (2) DIC increase at depth, and to (3) DIC and nutrient (nuts) reduction in the exported upper cell water. The effect of reduced NPP outside the SO dominates over the effect of reduced DIC and leads to (4) positive air-sea CO_2 flux anomalies (more outgassing or less uptake). An exception to that is the subpolar North Atlantic where the effect of reduced DIC dominates. (b) (5) Outgassing in the Southern Ocean leads to (6) reduced DIC content in the exported upper cell water, which can then (7) take up carbon outside the SO.

approach. We acknowledge that ocean circulation and biogeochemical feedbacks will further modify the carbon and nutrient distribution on the time scale of ocean circulation by a long-term redistribution of carbon and nutrients.

Physical pathways for carbon transfer to the deep ocean play an important role for carbon sequestration and are two orders of magnitude larger than other (biological) carbon fluxes in the mean state (Levy et al., 2013) and in their response to a perturbation of circulation (Hauck et al., 2013). We argue, however, based on our experiments, that a larger proportion of the carbon taken up via the biological pump re-emerges later than the carbon taken up via the physical carbon pump (Figure 8). The amount of carbon that is exported as detritus to below the mixed layer escapes the AAIW and SAMW route to the low latitudes' mixed layer. Even if this amount is smaller than the physically transported carbon, it reaches water masses that will not be reventilated as quickly as AAIW/SAMW and therefore contributes significantly to carbon sequestration. The physical transport of carbon is crucial and is also part of the biological carbon pump per se by transporting biological signals (e.g., upwelling of deep water which is rich in DIC due to remineralization of organic matter).

The "SO biogeochemical divide" identifies the AAIW/SAMW flow as the fast pathway determining nutrient availability in low latitudes and the AABW export as the slow pathway that is important for separating carbon

from the atmosphere on time scales of centuries (Marinov et al., 2006). The equatorward flux of SAMW and AAIW amounts to 8 Sv (Talley, 2013), whereas AABW contributes 29 Sv to the total flow toward the equator at 30°S (Talley, 2013). Our 200-year time scale does not capture the re-emergence of AABW to the global surface mixed layer. It is, however, clear that AABW transports a positive anomaly of biologically driven DIC (and nutrients) in contrast to the negative DIC anomaly in AAIW and SAMW (Figure 7). This decoupling facilitates the high efficiency of biologically driven carbon sequestration on the time scale considered here (Figure 8).

It is well established that upwelling of carbon-rich deep water in the SO in winter leads to oversaturation of surface pCO_2 (Bakker et al., 2016; Lenton et al., 2013; Mongwe et al., 2016; Takahashi et al., 2014) and to outgassing of CO_2 to the atmosphere. Our results are in accord with this process. However, the magnitude of the physical carbon flux out of the ocean might be overestimated by keeping the atmospheric CO_2 concentration constant and thereby allowing the ocean to reach quasi-equilibrium with the atmosphere. In the real world, atmospheric CO_2 concentration is not steady, but constantly increasing (Le Quéré et al., 2018) resulting in an increasing ocean-atmosphere CO_2 gradient that works toward less outgassing/more CO_2 uptake by the ocean. A second experimental setup with increasing atmospheric CO_2 concentration, however, illustrated that this complicates the interpretation as the SO turns from abiotically driven outgassing to abiotically driven uptake as the atmospheric CO_2 becomes larger than the deep water pCO_2. Furthermore, a water parcel transported out of the SO and being upwelled in low latitudes is in contact with a different atmospheric CO_2 concentration than at the time of subduction. Nevertheless, this second experiment demonstrates how strongly the effect of SO air-sea CO_2 exchange on lower latitudes depends on the atmospheric CO_2 disequilibrium in the SO (see also DeVries & Primeau, 2009) and on the history thereof in the AAIW/SAMW.

Our results are based on one marine biogeochemical model and will be model dependent, as biological model uncertainty is generally high (Laufkötter et al., 2015, 2016). For primary productivity, the compensation value is sensitive to the biological formulation because changes in biological functioning can impact the cycling of nutrients in the upper ocean independent of the nutrient supply. For example, more nutrient recycling in the upper ocean outside of the SO could occur to increase the compensation value. The model does not consider ballasting and applies one sinking velocity (increasing with depth) to the one detritus class. The simulated shift between nanophytoplankton and diatoms outside the SO might trigger changes in export and transfer efficiencies which are not considered. Nevertheless, we consider the results for export production and CO_2 flux to be more robust than surface primary productivity, as a key part of the simulated response is the redistribution of nutrients and carbon in the ocean by biological processes. It is well established that the SO is a high-nutrient-low-chloropohyll region (e.g., de Baar et al., 1990; Smetacek et al., 2012) that leaks macronutrients to lower latitude regions. Similarly, the trapping of nutrients in the SO with active biology is a feature of the SO circulation and the remineralization of sinking organic matter (Holzer & Primeau, 2013; Holzer et al., 2014). This mechanism provides a positive feedback on SO export production by increasing the nutrient concentrations of the upwelled water and effectively trapping nutrients in the SO (Holzer et al., 2014). When SO biology is turned off, the nutrients move out of the SO, but there is much less nutrient trapping outside the SO linking export production with resupply, which reduces the compensation. Our control simulation results in reasonable surface distributions and vertical gradients of nutrients and carbon as shown in previous evaluations of the same model (Hauck et al., 2013, 2016), confirming that we capture the important mechanisms for SO biogeochemistry such as nutrient trapping. Furthermore, the anomalies of nutrient distributions are supported by recent interpretation of the ocean overturning and radiocarbon data (De Lavergne et al., 2017).

5. Concluding Remarks

With this set of idealized simulations, we aimed to provide a framework that can be used to relate changes in the SO carbon pumps to large-scale changes in biogeochemistry and carbon cycle. The biological carbon pump in the SO is more efficient in storing carbon in the ocean interior than the physical carbon pump. Both carbon pumps in the SO have large impacts on remote carbon fluxes, but with reverse sign. A perturbation of one without the other may alter global carbon fluxes considerably. While abiotically driven CO_2 uptake might be balanced within 200 years, potential future changes in the biological carbon pump will impact the global carbon cycle for much longer. Ongoing circulation changes and increasing atmospheric CO_2 concentration may further modify the described connection between the SO and the global nutrient and carbon cycles. SO air-sea CO_2 exchange driven by abiotic processes is to 90% compensated outside of the SO. An active SO biological carbon pump leads to export production and air-to-sea CO_2 flux in the SO of which only 50% are compensated outside of the SO. This suggests that it is the noncompensated fraction of net primary/export

production that largely sets this CO_2 response outside of the SO. While diatom production is to 90% compensated outside the SO, nanophytoplankton production is not compensated and this shift is responsible for the incomplete compensation of SO production and air-sea CO_2 exchange.

Acknowledgments
We thank the editor and two anonymous reviewers for their constructive feedback. This research was supported under Australian Research Council's Special Research Initiative for Antarctic Gateway Partnership (Project ID SR140300001) and under the Initiative and Networking Fund of the Helmholtz Association (Helmholtz PostDoc programme, grant number PD-102, and Helmholtz Young Investigator Group Marine Carbon and Ecosystem Feedbacks in the Earth System (MarESys), grant number VH-NG-1301. The REcoM model code used for this publication can be downloaded from https://swrepo1.awi.de/projects/recom/ after registration. This code runs with the MITgcm checkpoint 65n available from mitgcm.org. The model results can be downloaded from https://doi.pangaea.de/10.1594/PANGAEA.894686.

References

Ayers, J. M., & Strutton, P. G. (2013). Nutrient variability in Subantarctic Mode Waters forced by the Southern Annular Mode and ENSO. *Geophysical Research Letters*, *40*, 3419–3423. https://doi.org/10.1002/grl.50638

Bakker, D. C. E., Pfeil, B., Landa, C. S., Metzl, N., O'Brien, K. M., Olsen, A., et al. (2016). A multi-decade record of high-quality fCO_2 data in version 3 of the Surface Ocean CO_2 Atlas (SOCAT). *Earth System Science Data*, *8*(2), 383–413. https://doi.org/10.5194/essd-8-383-2016

Behrenfeld, M. J., & Milligan, A. J. (2013). Photophysiological expressions of iron stress in phytoplankton. *Annual Review of Marine Science*, *5*, 217–246. https://doi.org/10.1146/annurev-marine-121211-172356

Bopp, L., Resplandy, L., Orr, J. C., Doney, S. C., Dunne, J. P., Gehlen, M., et al. (2013). Multiple stressors of ocean ecosystems in the 21st century: Projections with CMIP5 models. *Biogeosciences*, *10*(10), 6225–6245. https://doi.org/10.5194/bg-10-6225-2013

Brzezinski, M. A., Pride, C. J., Franck, V. M., Sigman, D. M., Sarmiento, J. L., Matsumoto, K., et al. (2002). A switch from $Si(OH)_4$ to NO_3^- depletion in the glacial Southern Ocean. *Geophysical Research Letters*, *29*(12), 1564. https://doi.org/10.1029/2001GL014349

de Baar, H. J., Buma, A. G., Nolting, R. F., Cadée, G. C., Jacques, G., & Tréguer, P. J. (1990). On iron limitation of the Southern Ocean: Experimental observations in the Weddell and Scotia Seas. *Marine ecology progress series*, 105–122.

De Lavergne, C., Madec, G., Roquet, F., Holmes, R., & McDougall, T. (2017). Abyssal ocean overturning shaped by seafloor distribution. *Nature*, *551*(7679), 181–186. https://doi.org/10.1038/nature24472

DeVries, T., Holzer, M., & Primeau, F. (2017). Recent increase in oceanic carbon uptake driven by weaker upper-ocean overturning. *Nature*, *542*(7640), 215–218. https://doi.org/10.1038/nature21068

DeVries, T., & Primeau, F. (2009). Atmospheric pCO_2 sensitivity to the solubility pump: Role of the low-latitude ocean. *Global Biogeochemical Cycles*, *23*, GB4020. https://doi.org/10.1029/2009GB003537

DeVries, T., Primeau, F., & Deutsch, C. (2012). The sequestration efficiency of the biological pump. *Geophysical Research Letters*, *39*, L13601. https://doi.org/10.1029/2012GL051963

Dlugokencky, E., & Tans, P. (2016). Trends in atmospheric carbon dioxide. National Oceanic & Atmospheric Administration, Earth System Research Laboratory (NOAA/ESRL). Retrieved from http:// www.esrl.noaa.gov/gmd/ccgg/trends/global.html, last access: 28 October 2016.

Downes, S. M., Langlais, C., Brook, J. P., & Spence, P. (2017). Regional impacts of the westerly winds on Southern Ocean mode and intermediate water subduction. *Journal of Physical Oceanography*, *47*(10), 2521–2530. https://doi.org/10.1175/JPO-D-17-0106.1

Dufour, C. O., Sommer, J. L., Gehlen, M., Orr, J. C., Molines, J., Simeon, J., & Barnier, B. (2013). Eddy compensation and controls of the enhanced sea-to-air CO_2 flux during positive phases of the Southern Annular Mode. *Global Biogeochemical Cycles*, *27*, 950–961. https://doi.org/10.1002/gbc.20090

Frölicher, T. L., Sarmiento, J. L., Paynter, D. J., Dunne, J. P., Krasting, J. P., & Winton, M. (2015). Dominance of the Southern Ocean in anthropogenic carbon and heat uptake in CMIP5 models. *Journal of Climate*, *28*(2), 862–886. https://doi.org/10.1175/JCLI-D-14-00117.1

Geider, R. J., MacIntyre, H. L., & Kana, T. M. (1998). A dynamic regulatory model of phytoplankton acclimation to light, nutrients, and temperature. *Limnology and Oceanography*, *43*, 679–694. https://doi.org/10.4319/lo.1998.43.4.0679

Gruber, N., Gloor, M., Mikaloff Fletcher, S. E., Doney, S. C., Dutkiewicz, S., Follows, M. J., et al. (2009). Oceanic sources, sinks, and transport of atmospheric CO_2. *Global Biogeochemical Cycles*, *23*, GB1005. https://doi.org/10.1029/2008GB003349

Hauck, J., Köhler, P., Wolf-Gladrow, D., & Völker, C. (2016). Iron fertilisation and century-scale effects of open ocean dissolution of olivine in a simulated CO_2 removal experiment. *Environmental Research Letters*, *11*(2), 024007. https://doi.org/10.1088/1748-9326/11/2/024007

Hauck, J., & Völker, C. (2015). Rising atmospheric CO_2 leads to large impact of biology on Southern Ocean CO_2 uptake via changes of the Revelle factor. *Geophysical Research Letters*, *42*, 1459–1464. https://doi.org/10.1002/2015GL063070

Hauck, J., Völker, C., Wang, T., Hoppema, M., Losch, M., & Wolf-Gladrow, D. A. (2013). Seasonally different carbon flux changes in the Southern Ocean in response to the southern annular mode. *Global Biogeochemical Cycles*, *27*, 1236–1245. https://doi.org/0.1002/2013GB004600

Hauck, J., Völker, C., Wolf-Gladrow, D. A., Laufkötter, C., Vogt, M., Aumont, O., et al. (2015). On the Southern Ocean CO_2 uptake and the role of the biological carbon pump in the 21st century. *Global Biogeochemical Cycles*, *29*, 1451–1470. https://doi.org/10.1002/2015GB005140

Holzer, M., & Primeau, F. W. (2013). Global teleconnections in the oceanic phosphorus cycle: Patterns, paths, and timescales. *Journal of Geophysical Research: Oceans*, *118*, 1775–1796. https://doi.org/10.1002/jgrc.20072

Holzer, M., Primeau, F. W., DeVries, T., & Matear, R. (2014). The Southern Ocean silicon trap: Data-constrained estimates of regenerated silicic acid, trapping efficiencies, and global transport paths. *Journal of Geophysical Research: Oceans*, *119*, 313–331. https://doi.org/10.1002/2013JC009356

Hoppema, M. (2004). Weddell Sea turned from source to sink for atmospheric CO_2 between pre-industrial time and present. *Global and Planetary Change*, *40*, 219–231. https://doi.org/10.1016/j.gloplacha.2003.08.001

Hoppema, M., Bakker, K., van Heuven, S. M., van Ooijen, J. C., & de Baar, H. J. (2015). Distributions, trends and inter-annual variability of nutrients along a repeat section through the Weddell Sea (1996–2011). *Marine Chemistry*, *177*, 545–553. https://doi.org/10.1016/j.marchem.2015.08.007

Iida, T., Odate, T., & Fukuchi, M. (2013). Long-term trends of nutrients and apparent oxygen utilization south of the polar front in Southern Ocean intermediate water from 1965 to 2008. *PloS One*, *8*(8), e71766. https://doi.org/10.1371/journal.pone.0071766

Ito, T., Woloszyn, M., & Mazloff, M. (2010). Anthropogenic carbon dioxide transport in the Southern Ocean driven by Ekman flow. *Nature*, *463*(7277), 80–83. https://doi.org/10.1038/nature08687

Jones, J. M., Gille, S. T., Goosse, H., Abram, N. J., Canziani, P. O., Charman, D. J., et al. (2016). Assessing recent trends in high-latitude southern hemisphere surface climate. *Nature Climate Change*, *6*(10), 917–926. https://doi.org/10.1038/nclimate3103

Jones, D. C., Meijers, A. J., Shuckburgh, E., Sallée, J.-B., Haynes, P., McAufield, E. K., & Mazloff, M. R. (2016). How does Subantarctic Mode Water ventilate the Southern Hemisphere subtropics? *Journal of Geophysical Research: Oceans*, *121*, 6558–6582. https://doi.org/10.1002/2016JC011680

Joos, F., & Spahni, R. (2008). Rates of change in natural and anthropogenic radiative forcing over the past 20,000 years. *Proceedings of the National Academy of Sciences*, *105*(5), 1425–1430.

Keeling, C. D., Bacastow, R. B., Bainbridge, A. E., Ekdahl, C. A. Jr., Guenther, P. R., Waterman, L. S., & Chin, J. F. (1976). Atmospheric carbon dioxide variations at Mauna Loa observatory, Hawaii. *Tellus*, *28*(6), 538–551.

Key, R. M., Kozyr, A., Sabine, C. L., Lee, K., Wanninkhof, R., Bullister, J. L., et al. (2004). A global ocean carbon climatology: Results from Global Data Analysis Project (GLODAP). *Global Biogeochemical Cycles*, *18*, GB4031. https://doi.org/10.1029/2004GB002247

Khatiwala, S., Primeau, F., & Hall, T. (2009). Reconstruction of the history of anthropogenic CO_2 concentrations in the ocean. *Nature*, *462*, 346–349. https://doi.org/10.1038/nature08526

Kobayashi, S., Ota, Y., Harada, Y., Ebita, A., Moriya, M., Onoda, H., et al. (2015). The JRA-55 Reanalysis: General specifications and basic characteristics. *Journal of the Meteorological Society of Japan Series II*, *93*(1), 5–48. https://doi.org/10.2151/jmsj.2015-001

Kriest, I., & Oschlies, A. (2008). On the treatment of particulate organic matter sinking in large-scale models of marine biogeochemical cycles. *Biogeosciences*, *5*(1), 55–72. https://doi.org/10.5194/bg-5-55-2008

Landschützer, P., Gruber, N., Haumann, F. A., Rödenbeck, C., Bakker, D. C., Van Heuven, S., et al. (2015). The reinvigoration of the Southern Ocean carbon sink. *Science*, *349*(6253), 1221–1224. https://doi.org/10.1126/science.aab2620

Langlais, C., Lenton, A., Matear, R., Monselesan, D., Legresy, B., Cougnon, E., & Rintoul, S. (2017). Stationary Rossby waves dominate subduction of anthropogenic carbon in the Southern Ocean. *Scientific Reports*, *7*(1), 17076. https://doi.org/10.1038/s41598-017-17292-3

Laufkötter, C., Vogt, M., Gruber, N., Aita-Noguchi, M., Aumont, O., Bopp, L., et al. (2015). Drivers and uncertainties of future global marine primary production in marine ecosystem models. *Biogeosciences*, *12*, 6955–6984. https://doi.org/10.5194/bg-12-6955-2015

Laufkötter, C., Vogt, M., Gruber, N., Aumont, O., Bopp, L., Doney, S. C., et al. (2016). Projected decreases in future marine export production: The role of the carbon flux through the upper ocean ecosystem. *Biogeosciences*, *13*(13), 4023–4047. https://doi.org/10.5194/bg-13-4023-2016

Le Quéré, C., Andrew, R. M., Friedlingstein, P., Sitch, S., Pongratz, J., Manning, A. C., et al. (2018). Global carbon budget 2017. *Earth System Science Data*, *10*(1), 405–448. https://doi.org/10.5194/essd-10-405-2018

Le Quéré, C., Rödenbeck, C., Buitenhuis, E. T., Conway, T. J., Langenfelds, R., Gomez, A., et al. (2007). Saturation of the Southern Ocean CO_2 sink due to recent climate change. *Science*, *316*, 1735–1738. https://doi.org/10.1126/science.1136188

Lenton, A., Tilbrook, B., Law, R., Bakker, D., Doney, S. C., Gruber, N., et al. (2013). Sea-air CO_2 fluxes in the Southern Ocean for the period 1990–2009. *Biogeosciences*, *10*, 4037–4054. https://doi.org/10.5194/bg-10-4037-2013

Leung, S., Cabré, A., & Marinov, I. (2015). A latitudinally banded phytoplankton response to 21st century climate change in the southern ocean across the cmip5 model suite. *Biogeosciences*, *12*(19), 5715–5734. https://doi.org/10.5194/bg-12-5715-2015

Levy, M., Bopp, L., Karleskind, P., Resplandy, L., Ethe, C., & Pinsard, F. (2013). Physical pathways for carbon transfers between the surface mixed layer and the ocean interior. *Global Biogeochemical Cycles*, *27*, 1001–1012. https://doi.org/10.1002/gbc.20092

MITgcm Group (2017). *MITgcm User Manual (online documentation)*. Cambridge, MA: MIT/EAPS. Retrieved from http://mitgcm.org/public/r2_manual/latest/online_documents/manual.html

Mahowald, N. M., Baker, A. R., Bergametti, G., Brooks, N., Duce, R. A., Jickells, T. D., et al. (2005). Atmospheric global dust cycle and iron inputs to the ocean. *Global Biogeochemical Cycles*, *19*, GB4025. https://doi.org/10.1029/2004GB002402

Marinov, I., Gnanadesikan, A., Toggweiler, J., & Sarmiento, J. (2006). The southern ocean biogeochemical divide. *Nature*, *441*(7096), 964–967. https://doi.org/10.1038/nature04883

Matsumoto, K., Sarmiento, J. L., & Brzezinski, M. A. (2002). Silicic acid leakage from the Southern Ocean: A possible explanation for glacial atmospheric pCO_2. *Global Biogeochemical Cycles*, *16*(3), 1031. https://doi.org/10.1029/2001GB001442

Mikaloff Fletcher, S. E., Gruber, N., Jacobson, A. R., Doney, S. C., Dutkiewicz, S., Gerber, M., et al. (2006). Inverse estimates of anthropogenic CO_2 uptake, transport, and storage by the ocean. *Global Biogeochemical Cycles*, *20*, GB2002. https://doi.org/10.1029/2005GB002530

Mikaloff Fletcher, S. E., Gruber, N., Jacobson, A. R., Gloor, M., Doney, S. C., Dutkiewicz, S., et al. (2007). Inverse estimates of the oceanic sources and sinks of natural CO_2 and the implied oceanic carbon transport. *Global Biogeochemical Cycles*, *21*, GB1010. https://doi.org/10.1029/2006GB002751

Mongwe, N. P., Chang, N., & Monteiro, P. M. (2016). The seasonal cycle as a mode to diagnose biases in modelled CO_2 fluxes in the Southern Ocean. *Ocean Modelling*, *106*, 90–103. https://doi.org/10.1016/j.ocemod.2016.09.006

Moore, J. K., Fu, W., Primeau, F., Britten, G. L., Lindsay, K., Long, M., et al. (2018). Sustained climate warming drives declining marine biological productivity. *Science*, *359*(6380), 1139–1143. https://doi.org/10.1126/science.aao6379

Morrison, A. K., Frölicher, T. L., & Sarmiento, J. L. (2015). Upwelling in the Southern Ocean. *Physics Today*, *68*(1), 27–32. https://doi.org/10.1063/PT.3.2654

Palter, J. B., Sarmiento, J. L., Gnanadesikan, A., Simeon, J., & Slater, R. D. (2010). Fueling export production: Nutrient return pathways from the deep ocean and their dependence on the Meridional Overturning Circulation. *Biogeosciences*, *7*(11), 3549–3568. https://doi.org/10.5194/bg-7-3549-2010

Panassa, E., Santana-Casiano, J. M., González-Dávila, M., Hoppema, M., van Heuven, S. M., Völker, C., et al. (2018). Variability of nutrients and carbon dioxide in the Antarctic Intermediate Water between 1990 and 2014. *Ocean Dynamics*, *68*(3), 295–308. https://doi.org/10.1007/s10236-018-1131-2

Pardo, P. C., Tilbrook, B., Langlais, C., Trull, T. W., & Rintoul, S. R. (2017). Carbon uptake and biogeochemical change in the Southern Ocean, south of Tasmania. *Biogeosciences*, *14*(22), 5217–5237. https://doi.org/10.5194/bg-14-5217-2017

Pasquier, B., & Holzer, M. (2016). The plumbing of the global biological pump: Efficiency control through leaks, pathways, and time scales. *Journal of Geophysical Research: Oceans*, *121*, 6367–6388. https://doi.org/10.1002/2016JC011821

Petit, J.-R., Jouzel, J., Raynaud, D., Barkov, N. I., Barnola, J.-M., Basile, I., et al. (1999). Climate and atmospheric history of the past 420,000 years from the Vostok ice core, Antarctica. *Nature*, *399*(6735), 429–436. https://doi.org/10.1038/20859

Primeau, F. W., Holzer, M., & DeVries, T. (2013). Southern Ocean nutrient trapping and the efficiency of the biological pump. *Journal of Geophysical Research: Oceans*, *118*, 2547–2564. https://doi.org/10.1002/jgrc.20181

Raven, J. A. (1988). The iron and molybdenum use efficiencies of plant growth with different energy, carbon and nitrogen sources. *New Phytologist*, *109*(3), 279–287.

Rodgers, K. B., Blanke, B., Madec, G., Aumont, O., Ciais, P., & Dutay, J.-C. (2003). Extratropical sources of Equatorial Pacific upwelling in an OGCM. *Geophysical Research Letters*, *30*(2), 1084. https://doi.org/10.1029/2002GL016003

Sallée, J.-B., Matear, R. J., Rintoul, S. R., & Lenton, A. (2012). Localized subduction of anthropogenic carbon dioxide in the Southern Hemisphere oceans. *Nature Geoscience*, *5*(8), 579–584. https://doi.org/10.1038/ngeo1523

Sarmiento, J., Gruber, N., Brzezinski, M., & Dunne, J. (2004). High-latitude controls of thermocline nutrients and low latitude biological productivity. *Nature*, *427*(6969), 56–60. https://doi.org/10.1038/nature02127

Sarmiento, J. L., & Orr, J. C. (1991). Three-dimensional simulations of the impact of Southern Ocean nutrient depletion on atmospheric CO_2 and ocean chemistry. *Limnology and Oceanography*, *36*(8), 1928–1950. https://doi.org/10.4319/lo.1991.36.8.1928

Shah, S. H. A. M., Primeau, F. W., Deleersnijder, E., & Heemink, A. W. (2017). Tracing the ventilation pathways of the deep North Pacific Ocean using Lagrangian particles and Eulerian tracers. *Journal of Physical Oceanography*, *47*(6), 1261–1280. https://doi.org/10.1175/JPO-D-16-0098.1

Smetacek, V., Klaas, C., Strass, V. H., Assmy, P., Montresor, M., Cisewski, B., et al. (2012). Deep carbon export from a Southern Ocean iron-fertilized diatom bloom. *Nature*, *487*(7407), 313–319. https://doi.org/10.1038/nature11229

Takahashi, T., Sutherland, S., Chipman, D., Goddard, J., Ho, C., Newberger, T., et al. (2014). Climatological distributions of pH, pCO_2, total CO_2, alkalinity, and $CaCO_3$ saturation in the global surface ocean, and temporal changes at selected locations. *Marine Chemistry*, *164*, 95–125. https://doi.org/10.1016/j.marchem.2014.06.004

Takahashi, T., Sutherland, S. C., Wanninkhof, R., Sweeney, C., Feely, R. A., Chipman, D. W., et al. (2009). Climatological mean and decadal change in surface ocean pCO_2, and net sea-air CO_2 flux over the global oceans. *Deep Sea Research Part II: Topical Studies in Oceanography*, *56*, 554–577. https://doi.org/10.1016/j.dsr2.2008.12.009

Talley, L. D. (2013). Closure of the global overturning circulation through the Indian, Pacific, and Southern Oceans: Schematics and transports. *Oceanography*, *26*(1), 80–97. https://doi.org/10.5670/oceanog.2013.07

Wetzel, P., Winguth, A., & Maier-Reimer, E. (2005). Sea-to-air CO_2 flux from 1948 to 2003: A model study. *Global Biogeochemical Cycles*, *19*, GB2005. https://doi.org/10.1029/2004GB002339

Williams, R. G., Roussenov, V., & Follows, M. J. (2006). Nutrient streams and their induction into the mixed layer. *Global Biogeochemical Cycles*, *20*, GB1016. https://doi.org/10.1029/2005GB002586